THE STRUCTURAL DESIGN OF TALL AND SPECIAL BUILDINGS
Struct. Design Tall Spec. Build. **23**, 995–1006 (2014)
Published online 30 July 2013 in Wiley Online Library (wileyonlinelibrary.com). DOI: 10.1002/tal.1101

Evaluation of seismic behavior improvement in RC MRFs retrofitted by controlled rocking wall systems

H. Zibaei[1,*,†] and J. Mokari[2]

[1]*Faculty of Engineering, Qom Branch, Islamic Azad university, Qom, Iran*
[2]*Department of Civil Engineering, Urmia University of Technology, Urmia, Iran*

SUMMARY

Using rocking wall systems is a recent technique to improve seismic behavior in reinforced concrete structures. This paper compares three 10-story and three 20-story reinforced concrete frames (moment-resisting frames) with intermediate ductility, reinforced concrete frames with shear wall, and reinforced concrete frames with controlled rocking wall (RCRW) by the use of pushover analysis. At the end of the research, the wall in a 20-story RCRW system is post-tensioned then analyzed, and its results were compared with RCRW results. Simulation and numerical analysis were performed with OpenSees software. The results show that plastic hinge formation and inter-story drifts are well distributed in the structure with rocking wall system in comparison with the other systems. Meanwhile, energy dissipation and displacement ductility are increased in RCRW frames. With post-tensioning wall in RCRW, the drift ratios are more uniformed. Copyright © 2013 John Wiley & Sons, Ltd.

Received 9 January 2013; Revised 29 May 2013; Accepted 12 June 2013

KEY WORDS: rocking wall; seismic behavior; OpenSees; post-tensioned tendon

1. INTRODUCTION

In the search for alternative structural systems that would sustain minor damage under strong earthquakes, researchers have studied rocking systems. At first, Housner (1963) investigated the free vibration response of a rigid rocking block. Then Meek (1975) studied the effects of structural flexibility rocking on foundation. After that, Aslam *et al*. (1980) realized that improvement of rocking resistance depends on anchoring a rigid structure to the ground and applying prestress in the anchor elements thereof. The concept of prestressing unbonded tendons in beam–column connection was proposed by Priestley and Tao (1993) and demonstrated through experimental work by Priestley and MacRae (1996). Kurama *et al*. (1998) described the performance of unbounded post-tensioned precast walls and subsequently suggested a seismic design methodology. Consequently, damage avoidance design (DAD) was introduced by Mander and Cheng (1997) who integrated the aspects of rocking, structural flexibility and prestressing in their DAD. Their methodology has attributes of both ductile design and seismic isolation. Ajrab *et al*. (2004) introduced implementation of proposed rocking shear walls as opposed to fixed-based walls in frame structures based on DAD philosophy, and rocking walls were coupled with a separate nonload bearing nonlinear supplemental damping system for improving seismic response. Supplemental system included prestressed tendons and energy dissipation devices. The comparison of two structures showed a reduction of floor accelerations inter-story drifts. Also, they conclude that the seismic response was not sensitive to wall width and to the prestress level in tendons. Wada *et al*. (2009) compared a retrofitting system of prestressed concrete rocking walls and steel dampers in a reinforced concrete frame against a moment-resisting frame (MRF). They deduced that in a rocking system without steel dampers, story drifts are reduced and

*Correspondence to: H. Zibaei, Faculty of Engineering, Qom Branch, Islamic Azad university, Qom, Iran
†E-mail: hosein.zibaei@civil.uut.ac.ir

uniformed. Setting up the steel dampers reduces the story drifts more. In this paper, pushover analysis is performed on three different structural system, that is, reinforced concrete frame (MRF), reinforced concrete frame with fixed base shear wall and reinforced concrete frame with rocking wall. The results are compared with each other. At first, the performance of a controlled rocking wall system under cyclic load is considered and validated with numerical model created by OPENSEES software.

2. VALIDATION OF A CONTROLLED ROCKING WALL UNDER CYCLIC LOADS

Preti *et al*. (2009) tested a full-scale prestressed rocking wall with unbounded tendons and unbounded steel dowels. Figure 1 shows the full-scale experimental test. The wall cross-section is $2800 \times 300\,mm^2$, and the wall height is 10 m. The lateral load is applied on the wall at a height of 8.8 m (Figure 1(a)). Unbounded steel dowels were adopted across the base cross-section in order to create adequate shear over-strength, whenever friction would lose due to local dynamic effects or damage. As shown in Figure 1(b), only horizontal stirrups are used in the wall in order to prevent concrete shear failure and crushing, and also eight unbounded tendons that consist of three 15-mm strands are replaced with the reinforcing longitudinal bars. The vertical loads (F_v, Figure 1(a)) are provided by post-tensioned tendons, which are 2500 kN in total. Steel pipes (steel dowels) are 48 mm in diameter and 8 mm in thickness and replace the sheaths of the cables at the base of the wall (Figure 1). It is noted that to avoid bond and thus axial stress in the dowels, they are wrapped in polythene sheaths. The confined concrete compressive strength is 55 MPa.

Figure 2 displays a schematic view of the methodology used for simulation of the experimental model in OPENSEES. The confined and unconfined concrete were considered by Kent–Scott–Park concrete model with degraded linear unloading/reloading stiffness according to the work of Karsan and Jirsa. In this model, Concrete 01 material (McKenna *et al*., 2006) is used for concrete fibers that assumed no tensile strength for concrete. The steel dowels are modeled using a reinforcing steel model named as ReinforcingSteel material (McKenna *et al*., 2006), which is specially intended to be used in a reinforced concrete fiber section as the steel reinforcing material. Moreover, the material of tendons is elastic-perfect plastic elements.

Unbounded steel dowels and unbounded tendons are modeled by truss element. Also, for modeling shear wall and rigid beams, nonlinear beam–column element and elastic beam–column elements are used. The wall is modeled to rock about its toes (Figure 2). This mechanism is done by applying compression only gap on rocking toes. The foundation is assumed rigid, so in order to create this condition, the modulus of elasticity of gaps is given as 10^{20}. Steel dowels are linked to the wall by rigid beam elements, and the connection is named X connection. As mentioned before, steel dowels are not

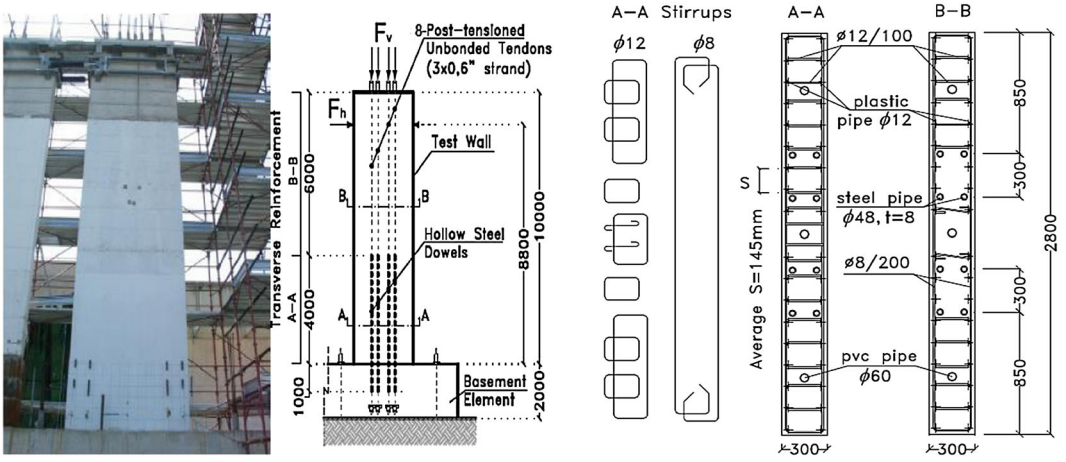

(a) Full scale experimental rocking wall (b) details of the wall

Figure 1. (a) Full-scale experimental rocking wall. (b) Plan of wall.

DOI: 10.1002/tal

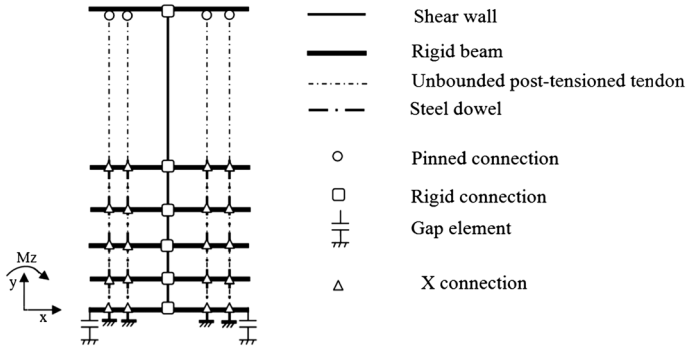

Figure 2. Analytical 2D model of rocking wall.

bonded to the wall and are just wrapped in sheaths. So it is assumed that steel dowels are displaced in the *x* direction of the wall and not linked to it in *y* and *Mz* directions (Figure 2, X connection).

The post-tensioning process of the tendons includes two steps, which are shown in Figure 3. The first step is applying post-tensioning to the tendons, and the second one is applying the loads that the post-tensioned tendons caused on the top of the wall.

This experimental test has two phases. The first one is with friction and the second one is without friction phase. An analysis is performed for the one with friction. Loading history on the test wall for the friction phase is applied at the top of the wall, which is summarized in Figure 4(a). Figure 4(b) compares the measured and predicted lateral load–top displacement response of the specimen indicating reliability of the analytical model.

3. PROTOTYPE STRUCTURES

Six structures are assessed in this study. Three structures are of 10 stories and three others 20 stories. The MRF and reinforced concrete frames with shear wall (RCSW) are designed and detailed in accordance with ACI 318-08 and lateral loading by Iranian seismic code (Building and Housing Research Center, 1999 Iranian Code of Practice for seismic resistant design of buildings. Standard

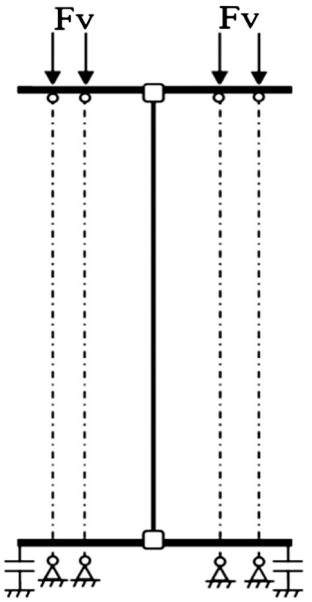

Figure 3. Applying loads on wall because of post-tensioning.

DOI: 10.1002/tal

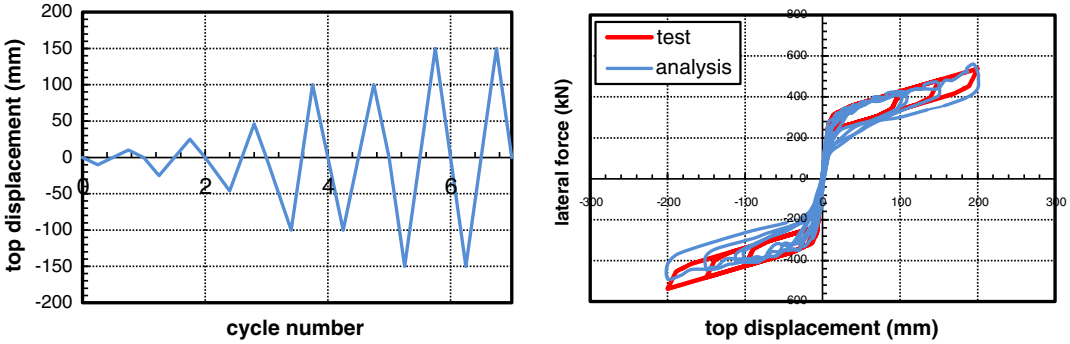

(a) Loading history on the test wall for the with friction phase.

(b) Hysteretic diagram of analytical and experimental results.

Figure 4. (a) Loading history on the test wall for the with friction phase. (b) Hysteretic diagram of analytical and experimental results.

No. 2800, 3rd edn), and the details of reinforced concrete frame with rocking wall (RCRW) are the same as RCSW one. All the structures are assumed to be lying on soil type II (medium dense sand or stiff clays). The plan dimensions of the structures are 12 m × 20 m. For all structures, the story height is 3.2 m. The system of the floor is assumed to be solid one-way slabs. Furthermore, the ductility of the frames is medium type. The plan of the prototype buildings is shown in Figure 5. The designed structures are assessed in BSE 1 (ground motion with a 10%/50-year exceedance probability). In Table 1, the beam, column and shear wall sections for each structure are shown.

4. ANALYTICAL MODEL

The concrete and steel materials are the same as those that are mentioned before. The compressive strength of confined concrete is assumed to be 25 MPa. The stress–strain relationship of confined and unconfined concrete is calculated following Paulay and Priestley (1992). The yield stress and ultimate strain of reinforcing steel is assumed to be 400 MPa and 0.12, respectively. The column and beam elements are modeled using a lumped plasticity approach, which in OpenSees is named as beam with hinges element (McKenna *et al.*, 2006). In these elements, the plasticity is concentrated at the ends of the element, and the extension of this region is called the plastic hinge length (L_p), which is a user-defined parameter. L_p is obtained from the following equation (Paulay and Priestley, 1992):

$$L_p = kL + 0.022F_y d_{bl} \tag{1}$$

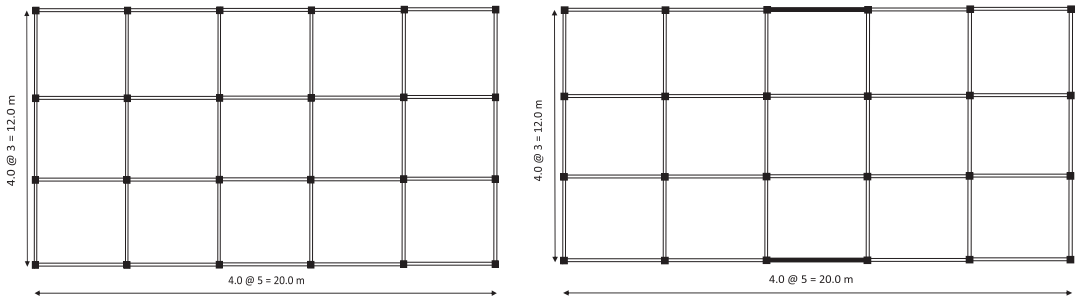

(a) (b)

Figure 5. (a) Plan of RC MRF. (b) Plan of RCSW, RCRW and RCPW.

DOI: 10.1002/tal

Table 1. Beam, column and shear wall sections for each structure.

Frame type	Story number	Beam ($m \times m$)	Column ($m \times m$)	Column reinf.	Shear wall	Shear wall reinf.
MRF—10 story	1–2	0.50×0.50	0.55×0.55	20Ø22	—	
	3–4	0.45×0.45	0.50×0.50	16Ø22	—	
	5–6	0.45×0.45	0.45×0.45	12Ø22	—	
	7–8	0.40×0.40	0.40×0.40	12Ø20	—	
	9–10	0.40×0.40	0.40×0.40	8Ø20	—	
RCSW—10 story	1–3	0.50×0.50	0.55×0.55	16Ø20	0.3×4.0	28Ø18
	4–6	0.45×0.45	0.50×0.50	12Ø20	0.3×4.0	20Ø18
	7–8	0.40×0.40	0.45×0.45	12Ø18	0.3×4.0	20Ø14
	9–10	0.40×0.40	0.40×0.40	12Ø18	0.2×4.0	16Ø12
MRF—20 story	1	0.50×0.50	0.70×0.70	24Ø25	—	
	2–5	0.50×0.50	0.70×0.70	24Ø22	—	
	6–9	0.45×0.45	0.65×0.65	24Ø22	—	
	10	0.45×0.45	0.60×0.60	20Ø22	—	
	11–14	0.45×0.45	0.55×0.55	16Ø22	—	
	15–16	0.45×0.45	0.50×0.50	16Ø20	—	
	17–20	0.40×0.40	0.45×0.45	12Ø20	—	
RCSW—20 story	1–2	0.45×0.45	0.65×0.65	24Ø22	0.5×4.0	33Ø25
	3–4	0.45×0.45	0.60×0.60	24Ø22	0.5×4.0	24Ø25
	5–10	0.45×0.45	0.60×0.60	20Ø22	0.4×4.0	20Ø20
	11–12	0.45×0.45	0.55×0.55	20Ø22	0.3×4.0	18Ø18
	13–16	0.45×0.45	0.50×0.50	16Ø20	0.3×4.0	18Ø18
	17–20	0.40×0.40	0.45×0.45	12Ø20	0.2×4.0	18Ø18

where

$$k = 0.2\left(\frac{F_u}{F_y} - 1\right) \leq 0.08 \tag{2}$$

and where d_{bl} is the longitudinal bar diameter, F_u is the ultimate steel strength and L is the length of the member.

Displacement-based beam–column elements are used for modeling shear walls. Meanwhile, the P-Delta effect is considered just for columns. In Figure 6, a 2D model of a rocking wall and shear wall in a three-bay and two-story frame is shown. Compression gap elements are used to create rocking motion for which a material with a relatively high modulus of elasticity (10^{20}) is defined to simulate the rigid floor assumption.

For modeling post-tensioned tendons, elastic-perfect plastic elements are used. The post-tensioning process of the tendons is the same as defined in the previous section. As mentioned before, two types of a 20-story RCRW system are modeled, which include with and without post-tensioned walls. For post-tensioning wall, there are two stages. The first stage is applying initial strain for tendons, and the second one is applying loads provided by tendons to the wall. When the wall is post-tensioned, the tendons provide two loads in opposite direction (Figure 7), and these loads are applied to the top and bottom of the wall.

After creating models in input files, gravity loads are applied. For all structures, the dead loads and live loads are assumed to be 6 and 2 kPa, respectively. The load combination of gravity loads that is used in this paper is $1.1(DL+LL)$ based on FEMA 356. Lateral load distribution is assumed to be triangular.

5. BI-LINEARIZATION PROCEDURE

After doing pushover analysis and plotting the capacity curve of structures, the bi-linear curves are extracted from them. Figure 8 shows the bi-linearization procedure. Considering this figure, K_i is initial stiffness of nonlinear curve, K_e is initial stiffness of bi-linear curve, Δ_y is yield displacement, V_y is

DOI: 10.1002/tal

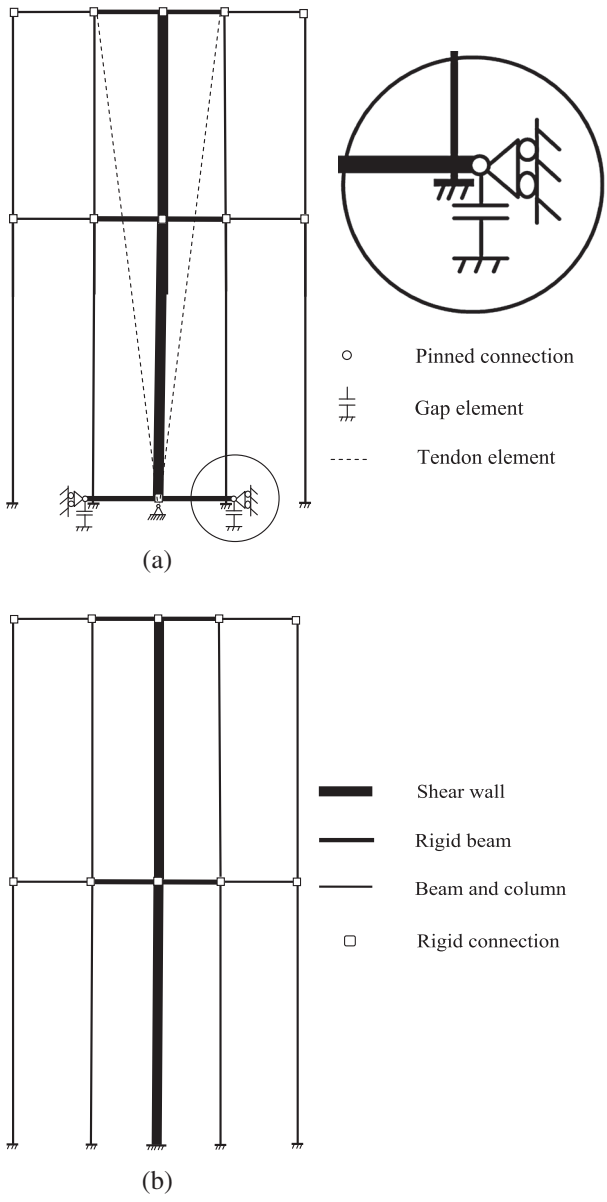

Figure 6. (a) Frame with rocking wall. (b) Frame with shear wall.

yield strength, Δ_m is maximum displacement corresponding to 20% strength reduction (FEMA 356) and V_m is maximum considered displacement.

One of the most important parameters that is considered is displacement ductility (μ). From Figure 8, μ is

$$\mu = \frac{\Delta_m}{\Delta_y} \tag{3}$$

6. PERFORMANCE LEVELS

On the basis of FEMA 356, there are three types of force–deformation curves for reinforced concrete structures components (Figure 9). Types 1 and 2 have ductile behavior, and the third one has brittle behavior. FEMA 356 suggests three performance levels for concrete structure components, which consist of immediate occupancy (IO), life safety (LS) and collapse prevention (CP). By extracting the outputs of the plastic hinge sections (their forces and deformations), the M–θ curve of each

DOI: 10.1002/tal

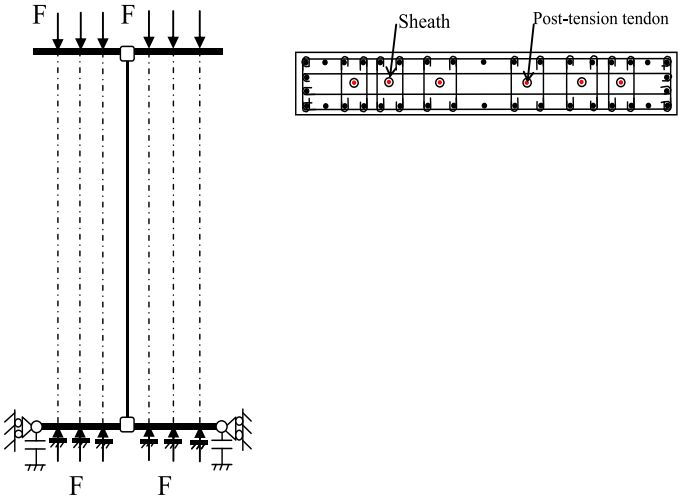

Figure 7. Applying post-tensioning loads on wall.

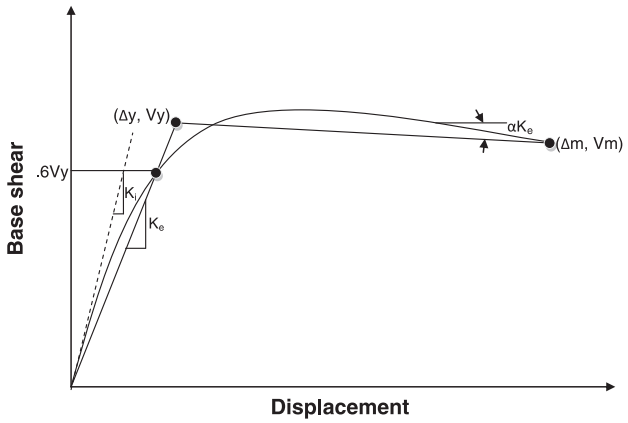

Figure 8. Bi-linear curve parameters.

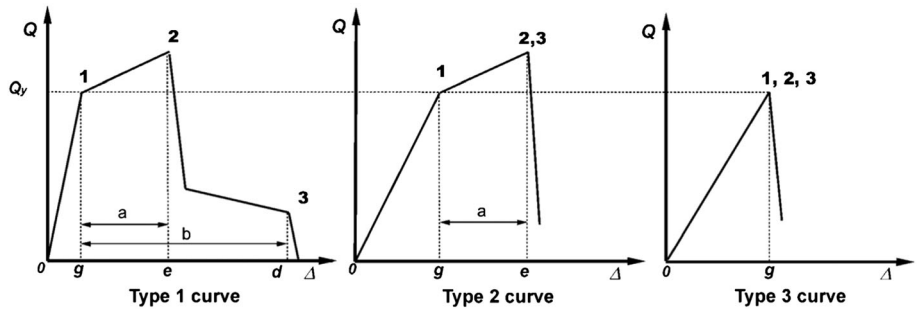

Figure 9. Component force versus deformation curves.

component is plotted. After that, with respect to the shape of the curve, the behavior of the component is determined, and then by referring to the tables of the suggested acceptance criteria (FEMA 356), the performance levels of the components are extracted.

DOI: 10.1002/tal

7. RESULTS

After doing pushover analysis based on FEMA 356, the force–displacement curve of each structure is plotted. Figure 10 displays a comparison of force–displacement curves and performance point of structures. According to this figure, it is obvious that base shear value of RCSW and RCRW is obtained about two times the corresponding value for the MRF structure. Another point that is considerable in Figure 10 is about sudden resistance reduction in RCSW structures. This event is investigated by plotting the base shear of the shear walls and the frames separately (Figure 11). As shown in this figure, the shear wall sudden failure is the reason of this resistance reduction.

In Table 2, the performance points of the structures have been given, and LS/IO and CP/IO ratios have been calculated. With respect to this table, the RCRW system has more LS/IO and CP/IO ratios compared with the other ones.

After creating bi-linear curves of each structure (Figure 12), bi-linear parameters of structures have been calculated and shown in Table 3. According to this table, the value of K_i obtained for RCSW is about 1.2 and 2 times the value of RCRW and MRF, respectively; and the value of K_e is approximately identical for RCSW and MRF systems. Also, the value of K_e for RCSW is about 1.1 times the value of RCRW. The next parameter that is considered in Table 2 is energy dissipation of frames. The value of energy dissipation for RCRW in contrast with MRF and RCSW is about 1.1 and 2 times.

The last parameter that is extracted from bi-linear curves is displacement ductility. This parameter is calculated and given in Table 4. By considering this table, ductility of RCRW is on average 1.3 and 1.32 times of RCSW and MRF, respectively.

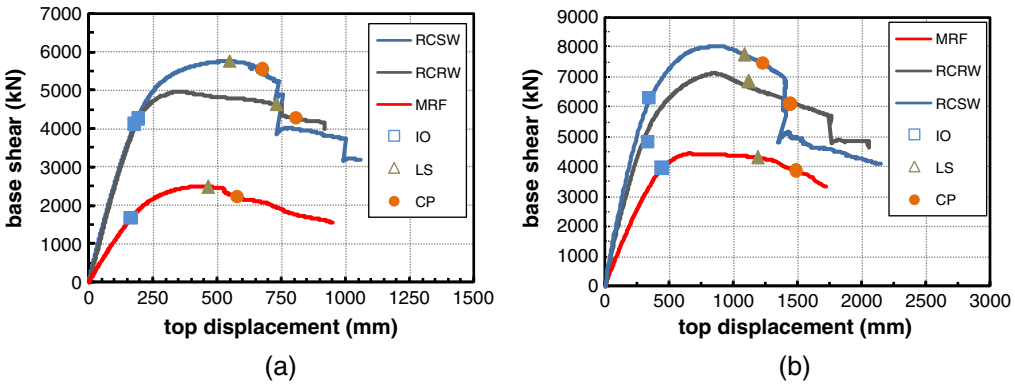

Figure 10. Performance level points of buildings: (a) 10 story, (b) 20 story.

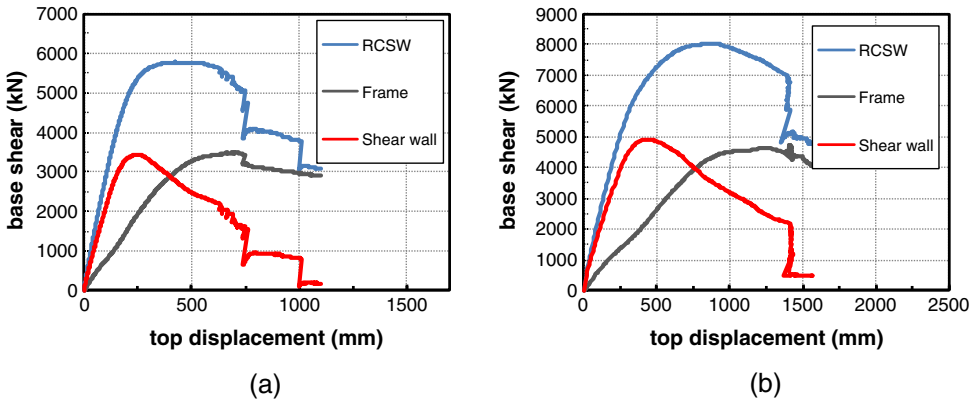

Figure 11. Base shear of frames and shear walls: (a) 10 story, (b) 20 story.

DOI: 10.1002/tal

Table 2. Performance levels of structures.

Story numbers	Frame type	IO (mm)	LS (mm)	CP (mm)	LS/IO	CP/IO
10 story	MRF	163.681	464.623	577.973	2.85	3.53
	RCSW	178.457	545.085	675.669	3.06	3.79
	RCRW	194.014	729.479	807.547	3.76	4.16
20 story	MRF	441.88	1190.544	1488.850	2.7	3.71
	RCSW	341.801	1084.320	1231.065	3.17	3.61
	RCRW	331.03	1119.87	1442.41	3.38	4.35

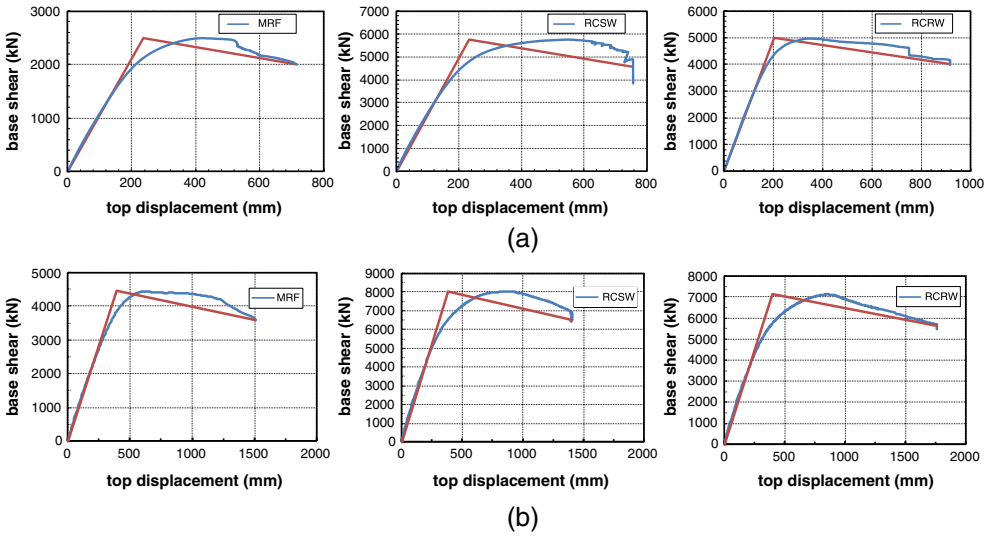

Figure 12. Pushover and bi-linear curves: (a) 10-story structures, (b) 20-story structures.

Table 3. The results of bi-linearization for prototype structures.

	Frame type	K_i (kN/mm)	K_e (kN/mm)	αK_e (kN/mm)	Energy (kN mm)
10 story	MRF	120.23	105.13	−1.02	1 371 885
	RCRW	326.78	246.34	−1.39	3 715 060
	RCSW	389.45	248.5	−2.25	3 353 275
20 story	MRF	172.14	112.45	−0.766	5 342 600
	RCRW	280.2	178	−1.08	10 107 600
	RCSW	339.12	211.2	−1.5	8 986 375

Table 4. Ductility comparison.

	Frame type	Δ_y (mm)	Δ_m (mm)	μ
10 story	MRF	237.01	714.1	3.01
	RCRW	203.52	915.0	4.5
	RCSW	232.5	750.25	3.23
20 story	MRF	395	1504	3.8
	RCRW	400	1780	4.45
	RCSW	380	1405	3.69

DOI: 10.1002/tal

The most important parameter that is considered is inter-story drifts. By using rocking wall system instead of shear wall, the inter-story drift of RCRW structures is properly distributed in all stories (Figure 13). This result shows that the distribution of plastic hinges in structure is to some extent

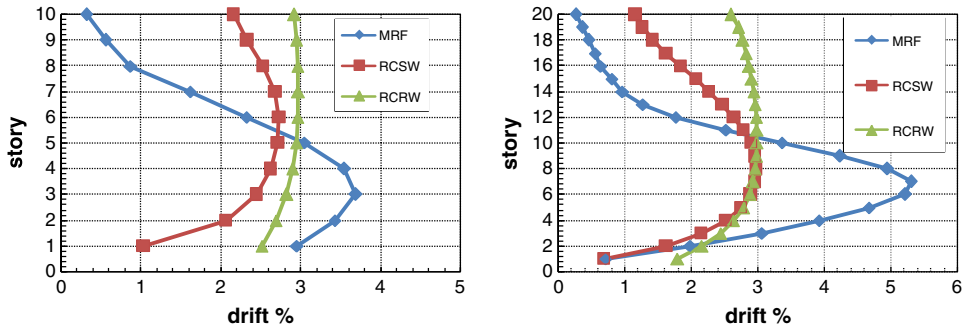

Figure 13. Story drifts of prototype structures in target displacement.

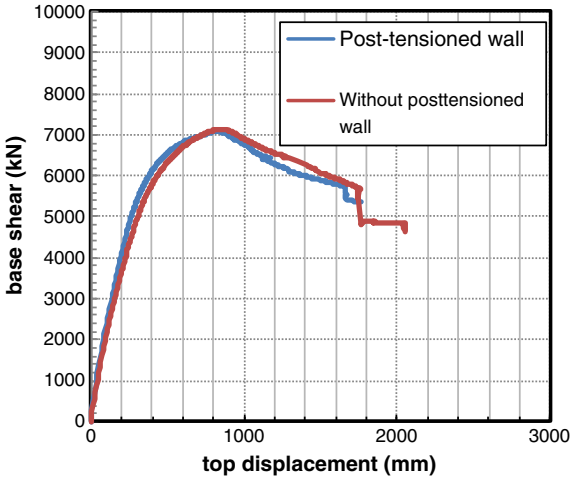

Figure 14. Pushover curves of 20-story RCRW system with and without post-tensioned walls.

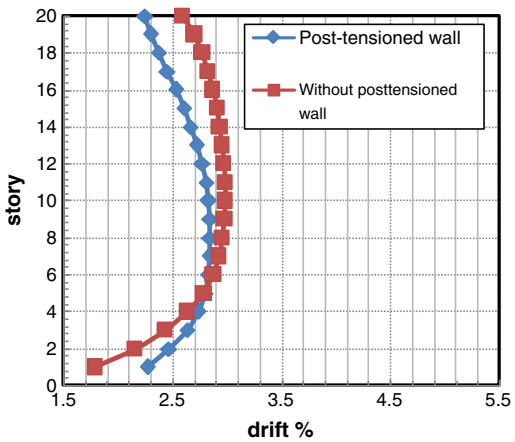

Figure 15. Story drifts of 20-story RCRW with and without post-tensioned walls.

DOI: 10.1002/tal

uniformed especially for a 10-story RCRW, so it seems that the wall in a 20-story RCRW needs to be retrofitted, and this is carried out by means of post-tensioning walls as defined before. Figure 14 displays base shear versus top displacement of 20 stories with and without post-tensioned wall, and there is approximately no difference between the curves. Of course, it is rational because by post-tensioning the wall, no lateral resistant system is added to the structure.

By considering Figure 15, for the post-tensioned wall system, the drift ratios are shifted from 2.25% up to 2.85% (drift variations are equal to $2.85 - 2.25 = 0.6$), whereas for the other one, the drift ratios are shifted from 1.79% up to 2.99% (drift variations is equal to $2.99 - 1.79 = 1.2$). Drift variations of RCRW system is 2 times those of RCRW with post-tensioned walls. So it is concluded that by retrofitting walls, the drift of stories are more uniformed (Figure 15).

8. CONCLUSIONS

This study investigates the advantages of using a rocking system in MRF structures. The results show that RCRW systems have more energy dissipation in contrast with RCSW and MRF systems. There is a sudden resistance reduction in RCSW structures because of shear wall failure, but in other prototype structures, this defect has not happened. Also, displacement ductility comparison of the structures shows a greater displacement ductility of RCRW models when compared with the other systems. It is noted that by using RCRW systems, drift ratios are more uniformly distributed, compared with those in RCSW and MRF systems. Also, it is concluded that by using rocking wall systems in MRF structures in order to retrofit them, a weak story mechanism is removed because of proper drift distribution. But for tall structures, it is needed to use post-tensioned or prestressed wall systems to obtain more uniform drift ratios. Meanwhile, MRF systems can be retrofitted by rocking wall systems by creating little change in foundation. It should be noted that one of the most significant problems in the event of an earthquake is uplift of foundation, which is somewhat removed in RCRW systems as the wall is not fixed to the base.

REFERENCES

Ajrab JJ, Pekcan G, Mander JB. 2004. Rocking wall-frame structures with supplemental tendon systems. *ASCE Journal of Structural Engineering* **130**(6): 895–903.

Aslam M, Goddon WG, Scalise DT. 1980. Earthquake rocking response of rigid bodies. *ASCE Journal of Structural Engineering* **106**(2): 377–392.

Building and Housing Research Center. 1999. *Iranian Code of Practice for seismic resistant design of buildings*. Standard No. 2800, 3rd edn, Building and Housing Research Center: Tehran, Iran

Housner GW. 1963. The behaviour of inverted pendulum structures during earthquake, *Bulletin of the Seismological Society of America* **53**(2): 403–417.

Kurama Y, Sause R, Pessiki S, Lu LW, El-Sheikh M. 1998. Seismic design and response evaluation of unbonded post-tensioned precast concrete walls. Precast Seismic Structural Systems (PRESSS). *Rep. No. 98/03*.

Mander JB, Cheng CT. 1997. Seismic resistance of bridge piers based on damage avoidance design. *Tech. Rep. NCEER-97-0014*, National Center for Earthquake Engineering Research, Buffalo, N.Y.

McKenna F, Fenves GL, Scott MH, Jeremić B. 2006. Open system for earthquake engineering simulation. http://opensees.berkeley.edu.

Meek JW. 1975. Effects of foundation tipping on dynamic response. *ASCE Journal of the Structural Division* **101**(7): 1297–1311.

Paulay T, Priestley MJN. 1992. *Seismic Design of Concrete and Masonry Buildings*, John Wiley Sons Inc. New York.

Preti M, Marini A, Metelli G, Giuriani E. 2009. Full scale experimental investigation on a prestressed rocking structural wall with unbonded steel dowels as shear keys. *ANIDIS Conf. on earthquake engineering, June and July, Bologna, Palazzo Re Enzo, Italy; 28–02*

Priestley MJN, MacRae GA. 1996. Seismic testing of precast beam-to-column joint assemblage with unbonded tendons. *PCI Journal, Precast/Prestressed Concrete Institute* **41**(1): 64–80.

Priestley MJN, Tao J. 1993. Seismic response of precast prestressed concrete frames with partially debonded tendons. *PCI Journal, Precast/Prestressed Concrete Institute* **38**(1): 58–69.

Wada A, Qu Z, Ito H, Motoyui S, Sakata H, Kasai K. 2009. *Seismic retrofit using rocking walls and steel dampers*. ATC/SEI Conference on Improving the Seismic Performance of Existing Buildings and Other Structures: San Francisco, CA, U.S.

DOI: 10.1002/tal

AUTHORS' BIOGRAPHIES

H. Zibaei is a supervisor in dwelling labor union of Qom city in Iran. He received his BS in Civil Engineering from the Faculty of Imam Mohmmad Baqer and his MS in Structural Engineering from Urmia University of Technology. His expertise includes nonlinear and dynamic analysis of structures and also simulation and analysis of pre-stress and post-tensioned structures.

J. Mokari has served as an Associate Professor of civil engineering at Urmia University of Technology and as a research associate at Urmia University since 2009. He is currently the head of Civil Engineering Department of Urmia University of Technology in Urmia. He received his MS and PhD in Structural Engineering from University of Tehran and International Institute of Earthquake Engineering and Seismology, respectively. He is a member of Iranian Earthquake Engineering Association and also member of graduation association of the Faculty of Engineering, University of Tehran.

DOI: 10.1002/tal